



Mesh-Based Design to Fabrication Workflows for Funicular Structures: A Case Study

Tommaso Casucci¹(✉), Ryan Hughes², Jens Pedersen³,
David Reeves⁴, Vishu Bhooshan¹, and Shajay Bhooshan¹

¹ Computational and Design Research Group (ZHCODE),
Zaha Hadid Architects, 10 Bowling Green Lane, London, England
tommaso.casucci@zaha-hadid.com

² Axis Consulting, Mejlgade 35B, 8000 Aarhus, Denmark

³ Odico Formwork Robotics, Peder Skrams Vej 5, 5220 Odense, Denmark

⁴ DNEG, 160 Great Portland Street, London, England

Abstract. Funicular shells have found large interest amongst architectural designers for their advantageous structural properties allowing them to cover large spans through the use of relatively weak and readily-available materials.

Although the properties of funicular structures are well-known and their efficiency well documented, the interdependencies of the multiple constraints present in real-world projects, from form-finding and rationalization to fabrication and assembly, mean that the realization of these structures remains a challenge.

This paper presents a unified design-to-fabrication workflow for funicular structures that adopts the Half-Edge (HE) mesh data structure throughout the entire design process from early-stage design to robotic fabrication.

The research contributes advancements in the fast early-stage design exploration of structure- and fabrication-aware proposals as well as the generation of voussoir geometry through mesh segmentation to the rationalization and documentation of geometric information for manufacturing and assembly.

The advancements are presented through the description of a case study, a proof-of-concept funicular vault manufactured using the Robotic Hot Wire Cutting (RHWC) method.

Keywords: Funicular design · Geometry processing · Half-Edge mesh · Stereotomy · Optimization · Robotic wire cutting

1 Introduction

The design of funicular shells have found a large and renewed interest within the field of architectural design due to their structural efficiency. Derived from geometrical principles rather than from material performance, these structures allow for the realization of relatively large spans that can be manufactured out of easily available materials working predominantly in compression (Fig. 1).



Fig. 1. Assembled pavilion inside the canteen of the Aarhus school of Architecture

Funicular shells construction often involves the production of large sets of unique, non-standard components – a problem to which the development of cost-effective solutions constitutes a significant area of research within the field of robotic and digital fabrication (RDF).

Although the design of funicular structures is a well documented field [1, 2], the multitude of constraints presented in real-world cases and their complex interdependencies – from form-finding and rationalization to fabrication and assembly mean that realization of these structures remains a challenge.

This paper demonstrates a design to fabrication workflow for funicular structures fabricated through robotic hot wire cutting (RHWC).

1.1 Related Work

While polygonal meshes are already quite popular in the early-stage phases of architectural projects, due to their conceptual simplicity, flexibility and efficiency of processing, a predominantly NURBS (Non-Uniform Rational B-Spline) based approach is still the accepted standard in later stages of the design process.

The friction generated by the two approaches is a common problem encountered in everyday architectural practice and often necessitates the potentially inefficient translation of geometrical information between the two data structures. Various solutions to bridge the two have previously been discussed [3, 4].

This paper presents a unified design to fabrication workflow for un-reinforced masonry vaults that utilizes the HE mesh data structure throughout the entire design process.

The generation of specific mesh topology for the purposes of form-finding that integrates aesthetic, structural, fabrication, assembly, sustainability and cost-related information has been previously investigated [5]. These methods focus on the generation of viable mesh topology based on an existing funicular solution. This paper

presents a practical method for the generation of suitable mesh topology starting from a user-defined un-directed graph. The method facilitates the fast, iterative exploration of structurally- and fabrication-aware design proposals that result in a near-optimal alignment of the mesh topology with the principle force direction through the funicular structure.

The stone cutting of masonry vaults historically involved a high level of expertise in the structural and geometric analysis of architectural forms. Advancements in the computational tessellation of free-form masonry vaults have been widely discussed [6, 7]. Common computational techniques generally involve some form of remeshing of the original form-found surface. We present a method based on mesh segmentation that avoids these re-meshing operations by taking advantage of the already near-optimal alignment of the mesh topology with the force flow.

Various robotic and digital fabrication strategies for the manufacturing of voussoirs have been previously discussed [8]. The advantages of RHWC with respect to alternative techniques have been presented in [9]. Through the implementation of the RHWC method, this paper describes a robotic manufacturing setup for the efficient production of six-sided voussoirs as well as an optimization strategy for the ruling count to prevent faceted surfaces and consequently minimize the finishing process.

The assembly of un-reinforced masonry vaults can invoke prohibitive costs due to the need for extensive temporary formwork. Alternative methods to overcome this problem have been prototyped, such as sets of sparse temporary chains [10]. This paper presents a method for the assembly of relatively large clusters of voussoirs in stable sections through the use of limited, local, temporary supports.

1.2 Project Overview

The prototypical structure has been designed, developed and assembled throughout the course of the Architectural Association (AA) Visiting School Aarhus in 2017 to frame the exhibition of the visiting school student projects. The overall dimensions of the structure are 4.50 m * 3.80 m by 2.90 m height.

2 Design

2.1 Form Finding and Topology Generation

A variety of simulation methods for the design and simulation of funicular shells have been previously described [11–13]. We chose to use a constraint-based solver implemented as described in [14] given the ability to consider multiple constraints (structural, dimensional, fabrication-related etc.) throughout the form finding process. A thrust surface is calculated by equalizing the sum of the forces derived by the constraints acting on the system.

We chose to generate the topology of the mesh to be used during the form-finding process through the thickening of an undirected graph. This method allows us to maintain a good degree of intuitive control over the starting geometry through a few control points at the ends of each segment while simultaneously resulting in a mesh

topology with a near-optimal alignment with the compressive forces in the structure for small offset values.

Figure 2 illustrates the construction of the mesh topology based on an input graph that can be edited by the user. Each face of the mesh is generated by calculating the angle bisector between adjacent edges and then offsetting graph edges by a user-defined distance. The resulting mesh is then subdivided using the Catmull-Clark algorithm to allow for smoother results throughout form finding.

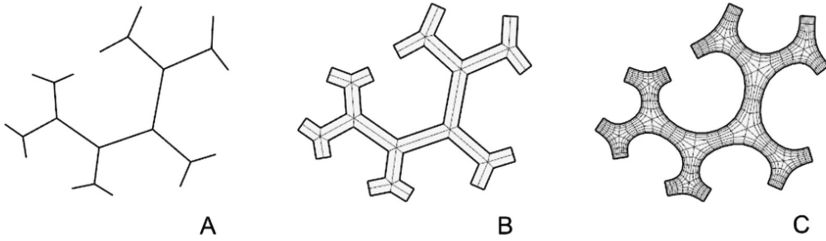


Fig. 2. Mesh modeling steps: (A) Graph, (B) Low polygon mesh, (C) Smooth Mesh

The ability of voussoirs to resist sliding and deformation is determined by the friction angle between the local force vector and the load-transferring faces between the voussoirs. The friction angle is defined as:

$$\tan \theta = \mu_s \tag{1}$$

where θ is the angle between the normal of the load-transferring face of the voussoir and the local force vector and μ_s is the static coefficient of friction between elements. For masonry μ_s varies between 0.60–0.70, which results in a friction angle of approximately 31°– 35°. The alignment of the mesh edges to the principal stress directions is shown in Fig. 3.

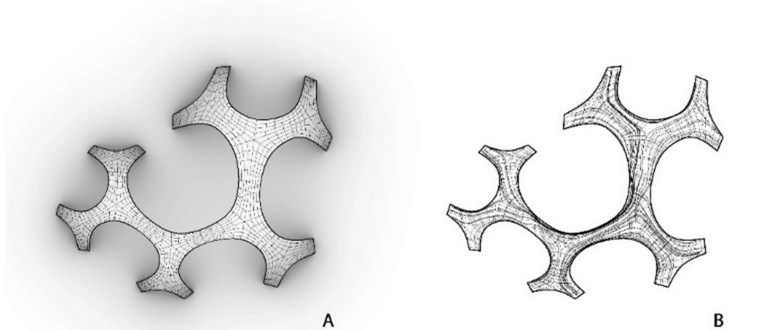


Fig. 3. Alignment of mesh edges (A) to principal stresses directions (B)

2.2 Voussoir Tessellation

Masonry structures depend on the assembly of multiple units to form a stable structural system that works in equilibrium through predominantly compression forces. The precise arrangement of individual elements is therefore of critical importance for the structural integrity of the structure [15].

The design of segmentation strategies that consider the multiple interdependencies of components of the design process such as structure, manufacturing and assembly is challenging. This section presents a discretization approach based on mesh-segmentation that integrates structural requirements as well as fabrication and assembly constraints.

For this task we take advantage of the HE mesh data structure [16] as it has significant advantages compared to its face-based counterpart such as that it allows for an arbitrary face-vertex count, the explicit representation of vertices, faces and edges and constant time connectivity information queries.

The form-found mesh is partitioned into smaller bands through the selection of loops of adjacent faces. The resulting bands are then re-built, removing all their clothed vertices. As a result, the bands become ruled and consequently ideally suitable for fabrication through RHWC.

The bands are then divided into smaller components by incrementally splitting along the ruling edges until the moment each band part fits the maximum available volume defined by the robotic setup described in Sect. 3.1 as well the maximum dimension of the available EPS stock material (1.2 m * 0.9 m * 0.9 m).

Both an aligned and mis-aligned splitting logic between adjacent bands have been considered. The misaligned option avoids the creation of continuous seams that cut through the structure and might reduce stability. The aligned option, however, is preferable in that it allows for the generation of easily-manageable clusters arranged around the structural nodes - largely advantageous at the assembly stages.

Tri-dimensional blocks are then generated by extruding the segmented mesh parts along the normals of the form-found geometry, with the thrust surface representing the central axis and the thickness being proportional to the compression forces in the block as described in [17].

The resulting contact faces of the voussoirs will be tangent to the thrust surface and therefore prevent instability through sliding action between voussoirs. As the extrusion operation does not add any clothed vertices within each voussoirs face we can also expect the thickened block geometry to be ruled (Fig. 4).

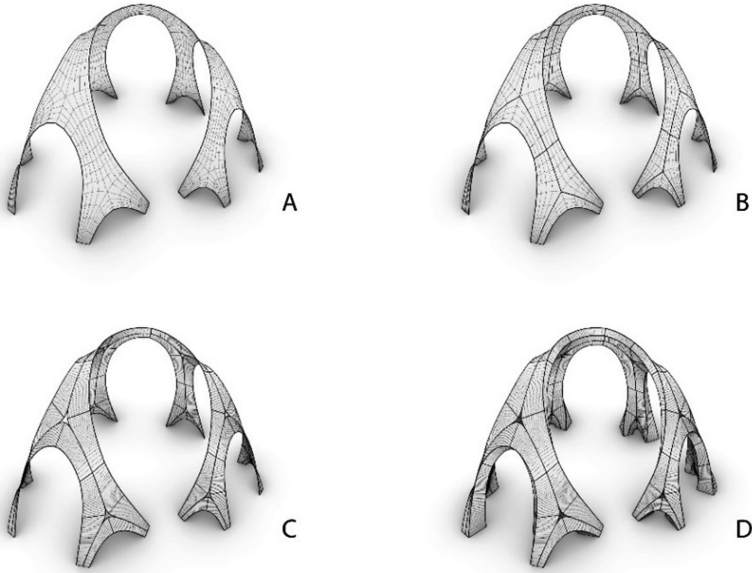


Fig. 4. Voussoir Tessellation: (A) Form Found Mesh, (B) Segmented Mesh, (C) Ruled Mesh, (D) Tri-dimensional voussoirs

3 Fabrication

3.1 Robot Setup

The voussoirs have been fabricated through a robotic hotwire cutting process. An insulated rectangular frame (Fig. 5) is mounted on the flange of an ABB IRB 6620 industrial robot, holding a pneumatically tensioned Nichrome wire with a diameter of 0.50 mm. Nichrome wire is particularly suitable for RHWC due to its high temperature coefficient of resistivity ($5.55 \Omega/m$) as well as its resistivity to corrosion and oxidation.

The wire is heated to a temperature of 200° and moved through the material, in this case expanded polystyrene (EPS) blocks with a compressive strength of 75 KN/m^2 and a melting point of 75° . The low density and melting point of the material enable a relatively high cutting speed of 20 mm per second, with the wire cutting along its entire axis simultaneously. In comparison with traditional digital mold manufacturing processes such as CNC milling, RHWC enables a dramatically higher rate of production.

The kinematic model, defined by the robot and tool construction, dictates the maximum tool reach and consequently the maximum permissible fabrication volume. Cutting ruled surfaces on all six sides of a three-dimensional geometry requires movement within a relatively expansive area - even larger robot models such as the one used here fail to easily maneuver to all the necessary target positions. The solution implemented in this project to minimize reachability issues relied on two primary components: the careful motion planning of the cut routines and the use of an additional external axis.

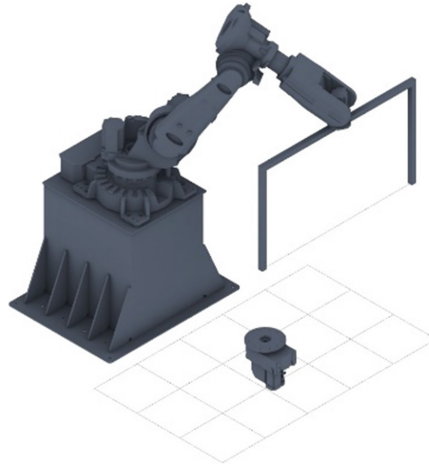


Fig. 5. Robotic hot wire cutting setup consisting of an ABB IRB 6620 industrial robot mounted on a platform, holding a hotwire cutter measuring $1.8 \text{ m} \times 1.05 \text{ m}$ and an external rotary axis

The tool has been calibrated using a calibration plane centered at the midpoint of the wire, with the Y-Axis parallel to the wire and the Z-Axis perpendicular to the robot flange frame Z-Axis. Thus, the wire acts as a tool with two degrees of freedom (DOF) - both around and along its Y-Axis, with some flexibility in the position of the target along the wire and a possibility to rotate the wire to improve the robot flange position.

3.2 Material Optimization

The use of expanded polystyrene foam in the creation of stereotomic voussoirs is largely considered a wasteful process. To minimize the amount of material used for each component, a comparative study was undertaken to assess various approaches to the optimization of the bounding box geometry used in the creation of stock material blocks.

The total material volume necessary to complete the structure was 1.58 m^3 . Traditional strategies consist of constraining material sizes to a fixed dimension from which all elements will be manufactured. Without further optimization, the application of this approach to the structure resulted in 18.86 m^3 of material, almost 12 times the necessary volume. Bounding boxes created in standard Cartesian space resulted in significantly improved material efficiency when compared to a standardized material size for all elements, but still required 9.5 m^3 , six times more than necessary (Fig. 6).

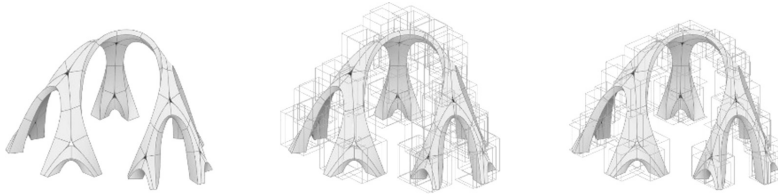


Fig. 6. Diagram showing the fabrication geometry (left), result of traditional standardization of stock material (center), result of Cartesian bounding box approach (right)

To reduce the amount of material required to a minimum it was necessary to compute the minimal bounding boxes in three-dimensional space. This was achieved using a principal component analysis (PCA) based on the edge networks of the components [18] (Fig. 7).

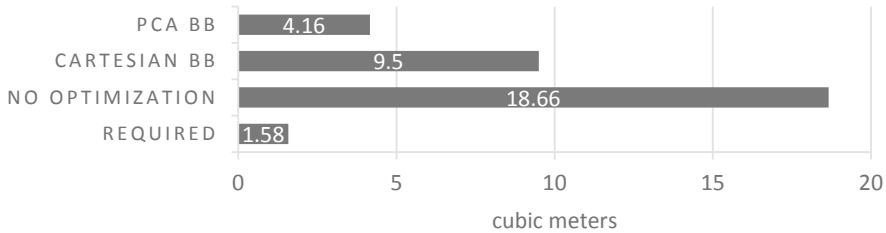


Fig. 7. Comparison of material optimization strategies with respect to the necessary bounding box material

The individual components of each mesh vertex were used to build dense 3-dimensional matrices. The Eigen-decomposition of these matrices resulted in the Eigen Vectors for each component, which were used to construct planes on which the minimal bounding boxes were created. Compared to the initial configuration, the minimal bounding boxes resulted in an average material reduction of 78%, with a total reduction of 14.7 m³ of material (Fig. 8).



Fig. 8. Diagram showing the fabrication geometry (left), planes generated using Principal Component Analysis (center), result of PCA-based bounding box approach (right)

3.3 Robotic Toolpath Generation

An asynchronous handshake strategy has been used to transfer geometry from the design and optimization model to the fabrication environment. The voussoir geometry, minimal bounding box geometry and the assembly information are distinctly grouped into element packages. The groups are subsequently oriented from design model space to the world origin plane through a change basis transformation, using the plane generated through the PCA as a reference position.

The geometry is then oriented from this base surface to the calibrated robot coordinate system where the rulings can be generated, and the wire orientation solved. The twisted nature of the component geometry prohibits traditional sorting strategies, whereby the mesh face normals are used to distinguish orientation and therefore cut ordering. Here, the HE mesh information is used to “walk” across the mesh from a starting position, pairing the ordered mesh edges to create rulings.

The mesh blocks are processed for fabrication in assembly order with the aim of minimizing the logistical complexity of storing and retrieving the components. Each block component consists of six faces comprised of ordered, non-planar quad mesh strips. Due to the careful prior construction of these mesh faces, rulings can be generated directly from the design model through the subdivision of each ordered pair of mesh edges to create linear rulings (Fig. 9).



Fig. 9. Diagram showing the oriented component geometry (left), initial clustering of mesh faces based on HE connectivity (center), result of ruling generation based on subdivision of ordered mesh edges (right)

Two opposing faces of the geometry are first cut, followed by a closed loop of the other four sides to minimize cut time and the complexity of the resultant voussoir.

Care has been taken to optimize the ruling count with respect to the fabrication process in question - if the resolution is too low the linear interpolation method used by the robot will result in visible facets on the surface of the components - if the resolution is too high, the approximation method used by the robot will fail and result in

vibrations, again distorting the final fabricated geometry. The shortest of the mesh edge pairs are segmented into 10 mm sections, and the division count is used to pair each point with an appropriate point on the matching edge.

The diameter of the wire and the chosen temperature dictate a radius around the target ruling through which it will remove material. If this is not compensated for, the resultant geometry will be significantly smaller than intended.

In addition to the need to offset all target wire positions to compensate for the effect radius of the wire, it is also important to consider cut direction when path planning. Due to the rising hot air generated by the wire, the method tends to remove slightly more material when cutting upwards along a geometry than downwards. Rather than introducing an additional geometric offset, the cutting speed is instead adapted to the cut direction to compensate for this effect.

3.4 Simulation

The digital robot setup, simulation and code generation was managed using Axis, a parametric robot control library for Grasshopper. The complexity of the robot reorientations and the large dimensions of the end-effector in relation to the robot resulted in a high probability for reachability issues and collisions. To manage this, a fast inverse kinematics approach was used to monitor the entire fabrication sequence in real time using simplified geometry. If reachability issues or collisions were found, the fabrication model attempted to automatically correct the robot program using the two degrees of freedom available in the tool. If no valid solutions could be found by rotating the wire around its axis, or if the resulting displacement of the robot flange was too large, an attempt was made to instead correct the program by moving the TCP along the ruling axis and re-interpolating the motion.

3.5 Fabrication

A complete digital model of the fabrication environment was created and used for a visual and more detailed kinematic simulation of the process as well as collision detection. Upon successful simulation of the fabrication process, the files were exported as RAPID modules and loaded to the robot controller. The average fabrication time for each component was eight minutes. A database was subsequently updated with information regarding the fabrication and assembly of the structure and used throughout the assembly process.

3.6 Assembly

The physical construction of self-supporting structures remains challenging, even at more manageable scales. Current construction processes require extensive formwork during assembly, which quickly leads to inflated construction costs and increased construction times.

A strategy of cluster-based assembly was chosen for the pavilion that enabled the gradual construction of the masonry model in stable sections without the need for complex temporary scaffolding.

Groups of component blocks have been clustered around the central nodes of each cluster of elements by taking advantage of the connectivity information stored into the HE mesh as shown in Fig. 10, with each cluster composed of six blocks.

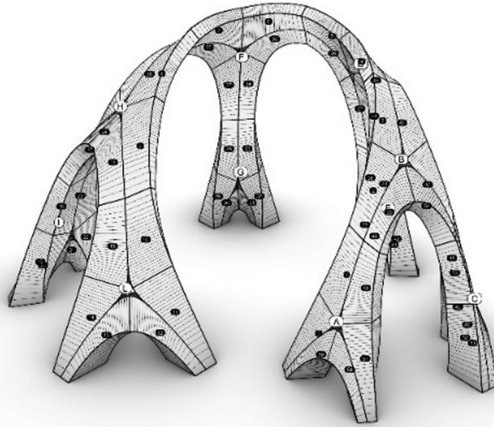


Fig. 10. Voussoir clustering

Once all blocks in a cluster have been cut these have been assembled together with the use of temporary connectors to form sub-assemblies. Arranging the blocks in clusters reduces the total number of individual elements to handle on-site in addition to making different sections of the structure easier to support during the assembly process. Each of the clusters have then been assembled on site with the help of a few local supports. The action of the temporary supports to counterbalance the part of the structure already in place is shown in Fig. 11.

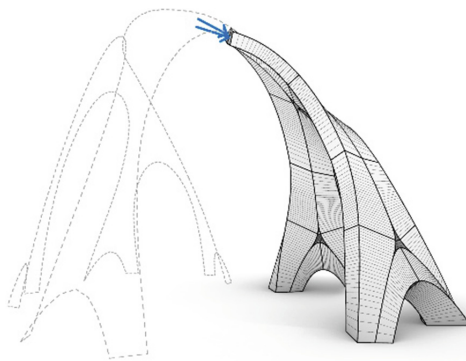


Fig. 11. Diagram showing the action of the temporary supports on the elements of the pavilion already in place during the assembling process

4 Conclusions

The paper presented a design to fabrication workflow for un-reinforced masonry vaults that utilizes the HE mesh data structure across the entire design process. The research contributes to the field with advancements in the fast early-stage design exploration of structure- and fabrication-aware proposals as well as the generation of voussoir geometry and the rationalization of geometric information for manufacturing, assembly and documentation.

A series of improvements to existing best practices in design to fabrication of funicular vaults are discussed:

- A graph-based topology generation method that allows for the fast, iterative exploration and intuitive editing of design proposals that maintain a constant and near-optimal alignment with compressive forces in the structure.
- A mesh segmentation-based voussoir tessellation strategy that considers the inter-dependencies between structural requirements, fabrication and assembly constraints.
- The implementation of a robotic fabrication setup for the efficient RHCW of six-sided voussoir geometry.
- Toolpath generation and ruling count optimization for the minimization of faced surface finishing.
- Material optimization through minimal bounding box that shows a reduction in material usage of 78% compared to traditional approaches.
- Node based assembly for the minimization logistical complexity and reduction of temporary scaffolding.

Finally, the feasibility of our approach was verified through the design and production of a proof-of-concept funicular prototype structure composed of RHCW EPS blocks.

References

1. Block, P.P.C.V.: Thrust network analysis: exploring three-dimensional equilibrium (2009)
2. Rippmann, M.: Funicular Shell Design - geometric approaches to form finding and fabrication of discrete funicular structures. ETH (2016)
3. Bhooshan, S.: Combining computer-aided geometry design and building information modelling. *AD Archit. Des.* **87**(3), 82–89 (2017)
4. Miller, N., Stasiuk, D.: A novel mesh-based workflow for complex geometry in BIM. In: *Disciplines and Disruption - Proceedings Catalog of the 37th Annual Conference of the Association for Computer Aided Design in Architecture, ACADIA 2017* (2017)
5. Oval, R., Rippmann, M., Mesnil, R., Van Mele, T., Baverel, O., Block, P.: Feature-based topology finding of patterns for shell structures. *Autom. Constr.* (2019)
6. Rippmann, M., Block, P.: Computational tessellation of freeform, cut-stone vaults. *Nexus Netw. J.* **20**, 545–566 (2018)
7. Rippmann, M., Block, P.: Digital stereotomy: voussoir geometry for freeform masonry-like vaults informed by structural and fabrication constraints. In: *IABSE-IASS2011* (2011)

8. Rippmann, M., et al.: The Armadillo Vault: computational design and digital fabrication of a freeform stone shell. In: *Advances in Architectural Geometry 2016*, pp. 344–363 (2016)
9. McGee, W., Feringa, J., Søndergaard, A.: Processes for an architecture of volume. In: *Rob| Arch 2012* (2013)
10. Deuss, M., et al.: Assembling self-supporting structures. *ACM Trans. Graph.* (2014)
11. Adriaenssens, S., Block, P., Veenendaal, D., Williams, C.: *Shell Structures for Architecture: Form Finding and Optimization* (2014)
12. Bhooshan, V., Reeves, D., Bhooshan, S., Block, P.: MayaVault—a mesh modelling environment for discrete funicular structures. *Nexus Netw. J.* **20**, 567–582 (2018)
13. Vouga, E., Höbinger, M., Wallner, J., Pottmann, H.: Design of self-supporting surfaces. *ACM Trans. Graph.* **31**, 87 (2012)
14. Deuss, M., Deleuran, A.H., Bouaziz, S., Deng, B., Piker, D., Pauly, M.: ShapeOp—a robust and extensible geometric modelling paradigm. In: *Modelling Behaviour* (2015)
15. Fallacara, G.: Toward a stereotomic design: experimental constructions and didactic experiences. In: *Proceedings of the Third International Congress on Construction History* (2009)
16. Botsch, M., Steinberg, S., Bischoff, S., Kobbelt, L.: OpenMesh - a generic and efficient polygon mesh data structure. In: *OpenSG Symposium* (2002)
17. Rippmann, M., Block, P.: Rethinking structural masonry: unreinforced, stone-cut shells. *Proc. Inst. Civil Eng.-Constr. Mater.* **166**, 378–389 (2013)
18. Jolliffe, I.T.: *Principal Component Analysis*, 2nd edn. (2002)